

Understanding the Ratio of the Partition Sum to its Bethe Approximation via Double Covers

Pascal O. Vontobel
*Department of Information Engineering
The Chinese University of Hong Kong
pascal.vontobel@ieee.org*

Abstract—For various classes of graphical models it has been observed that the ratio of the partition sum to its Bethe approximation is often close to being the square of the ratio of the partition sum to its degree-2 Bethe approximation. This is of relevance because the latter ratio can often better be analyzed and/or quantified than the former ratio. In this paper, we give some justifications for the observed relationship between these two ratios and then analyze these ratios for two classes of log-supermodular graphical models.

I. INTRODUCTION

The partition sum (a.k.a. the partition function) of a normal factor graph (NFG) N (see, e.g., [1]–[3]) is defined to be

$$Z(N) \triangleq \sum_{a \in \mathcal{A}} g(a). \quad (1)$$

Here, the sum is over the set of all configurations \mathcal{A} of N , and g is the global function of N . The relevance of the partition sum not only stems from the fact that it is an important quantity characterizing a graphical model, but also from the fact that many quantities of interest can be formulated as the partition sum of some suitable graphical model.

For many cases of interest, exactly computing the partition sum is intractable. Therefore, various techniques have been proposed to efficiently approximate the partition sum. For NFGs where the global function is a product of non-negative-valued local functions, a popular approach is to approximate $Z(N)$ by the Bethe partition sum $Z_B(N)$. The latter quantity is defined via the minimum of the Bethe free energy function [4] and for many graphical models it can be found efficiently with the help of the sum-product algorithm (SPA) [1], [3], [4].

The above definition of $Z_B(N)$ in terms of the minimum of the Bethe free energy function can be considered to be an analytical definition of $Z_B(N)$. On the other hand, as was shown in [5], $Z_B(N)$ can also be given a combinatorial characterization as follows:

$$Z_B(N) = \limsup_{M \rightarrow \infty} Z_{B,M}(N), \quad (2)$$

$$Z_{B,M}(N) \triangleq \sqrt[M]{\langle Z(\tilde{N}) \rangle_{\tilde{N} \in \tilde{\mathcal{N}}_M}}. \quad (3)$$

Here the expression under the root sign represents the (arithmetic) average of $Z(\tilde{N})$ over all M -covers \tilde{N} of N , $M \geq 1$. Note that for $M = 1$, the set $\tilde{\mathcal{N}}_M$ contains only the NFG N , and so

$$Z_{B,1}(N) = Z(N). \quad (4)$$

$$\begin{aligned} Z_{B,M}(N)|_{M \rightarrow \infty} &= Z_B(N) \\ | & \\ Z_{B,M}(N) & \\ | & \\ Z_{B,M}(N)|_{M=1} &= Z(N) \end{aligned}$$

Fig. 1: The degree- M Bethe partition sum of the NFG N for different values of M .

The results in (2)–(4) are summarized in Fig. 1. More details about the definition of NFGs and their graph covers will be given in Section II.

For various classes of NFGs it has been numerically and/or analytically observed that the following approximation holds:

$$\frac{Z(N)}{Z_B(N)} \approx \left(\frac{Z(N)}{Z_{B,2}(N)} \right)^2. \quad (5)$$

In this paper, we would like to argue that this is likely a general phenomenon. Note that (5) can also be rewritten as

$$Z_{B,2}(N) \approx \sqrt{Z(N) \cdot Z_B(N)}, \quad (6)$$

i.e., $Z_{B,2}(N)$ is approximately the geometric mean of the quantities $Z(N)$ and $Z_B(N)$. Eq. (5) can also be rewritten as

$$\rho(N) \triangleq \frac{Z(N) \cdot Z_B(N)}{(Z_{B,2}(N))^2} \approx 1. \quad (7)$$

The expression in (5) is of relevance because, while the ratio on the LHS of (5) is of interest, the ratio on the RHS of (5) can often be better analyzed and/or quantified.

Let us discuss a case where the approximate equality in (5) was observed. Namely, let \mathbf{A} be the all-one matrix of size $n \times n$ for an arbitrary positive integer n . It was shown in [6] and in [7], respectively, that¹

$$\frac{\text{perm}(\mathbf{A})}{\text{perm}_B(\mathbf{A})} \sim \sqrt{\frac{2\pi n}{e}}, \quad (8)$$

$$\frac{\text{perm}(\mathbf{A})}{\text{perm}_{B,2}(\mathbf{A})} \sim \sqrt[4]{\frac{\pi n}{e}}. \quad (9)$$

Observe that, up to a factor $\sqrt{2}$, the relationship in (5) is essentially satisfied for large n .

¹The notation $a(n) \sim b(n)$ stands for $\lim_{n \rightarrow \infty} \frac{a(n)}{b(n)} = 1$.

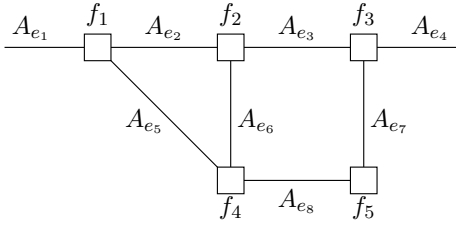


Fig. 2: NFG \mathbf{N} used in Example 1.

A. Overview

The paper is structured as follows. In Section II we give a brief introduction to NFGs and their double covers. In Section III we justify the approximate equality in (5). In Sections IV and V we analyze $\rho(\mathbf{N})$ for two classes of NFGs, first a very simple class and then a more sophisticated class consisting of log-supermodular graphical models. Finally, in Section VI we conclude the paper.

II. NORMAL FACTOR GRAPHS AND THEIR FINITE COVERS

Factor graphs are a convenient way to represent the factorization of multivariate functions [1]. Normal factor graphs (NFGs) [2], also called Forney-style factor graphs [3], are a variant of factor graphs where variables are associated with edges. The following example is taken from [5].

Example 1. Consider the multivariate function

$$g(a_{e_1}, \dots, a_{e_8}) \triangleq f_1(a_{e_1}, a_{e_2}, a_{e_5}) \cdot f_2(a_{e_2}, a_{e_3}, a_{e_6}) \cdot f_3(a_{e_3}, a_{e_4}, a_{e_7}) \cdot f_4(a_{e_5}, a_{e_6}, a_{e_8}) \cdot f_5(a_{e_7}, a_{e_8}),$$

where the so-called global function g is the product of the so-called local functions f_1, f_2, f_3, f_4 , and f_5 . The decomposition of this global function as a product of local functions can be depicted with the help of an NFG \mathbf{N} as shown in Fig. 2. In particular, the NFG \mathbf{N} consists of

- the function nodes f_1, f_2, f_3, f_4 , and f_5 ;
- the half edges e_1 and e_4 (sometimes also called “external edges”);
- the full edges e_2, e_3, e_5, e_6, e_7 , and e_8 (sometimes also called “internal edges”).

In general,

- a function node f represents the local function f ;
- with an edge e we associate the variable A_e (note that a realization of the variable A_e is denoted by a_e);
- an edge e is incident on a function node f if and only if a_e appears as an argument of the local function f .

Finally, we associate with \mathbf{N} the partition sum $Z(\mathbf{N})$ as defined in (1). (Note that we do not consider any temperature dependence of $Z(\mathbf{N})$ in this paper.)

Throughout this paper, we will essentially use the same notation as in [5]. The only exceptions are $Z(\mathbf{N})$ instead of $Z_G(\mathbf{N})$ for the partition sum, and f instead of g_f for local functions. (For notations which are not defined in this paper, we refer the reader to [5].) Note that for the rest of this paper,

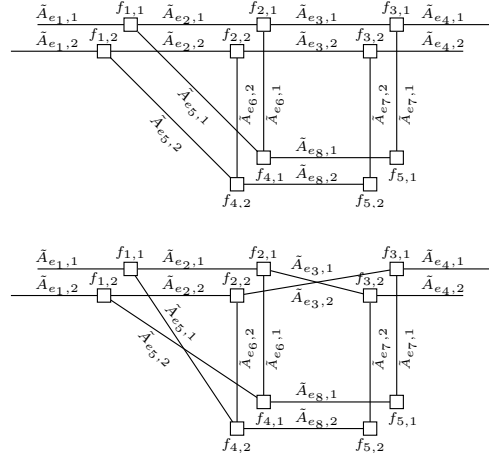


Fig. 3: Two possible 2-covers of the NFG \mathbf{N} in Fig. 2.

we assume that local functions in the base NFG \mathbf{N} take on only non-negative real values, *i.e.*, $f(\mathbf{a}_f) \in \mathbb{R}_{\geq 0}$ for all f and all \mathbf{a}_f . However, transformations of \mathbf{N} might have local functions that take on negative real values.

Central to this paper are also finite graph covers of an NFG. (For the definition of a finite graph cover, see, *e.g.*, [5].) The following example is taken from [5].

Example 2. Consider again the NFG \mathbf{N} that is discussed in Example 1 and depicted in Fig. 2. Two possible 2-covers of this (base) NFG are shown in Fig. 3. The first graph cover is “trivial” in the sense that it consists of two disjoint copies of the NFG in Fig. 2. The second graph cover is “more interesting” in the sense that the edge permutations are such that the two copies of the base NFG are intertwined. (Of course, both graph covers are equally valid.)

Based on finite graph covers, one can define the degree- M Bethe partition sum $Z_{B,M}(\mathbf{N})$ as in (3) for any $M \geq 1$. With this, one can prove the alternative expression for $Z_B(\mathbf{N})$ in (2). When considering the value of $Z_{B,M}(\mathbf{N})$ from $M = 1$ to $M = \infty$, one goes from $Z(\mathbf{N})$ to $Z_B(\mathbf{N})$ as shown in Fig. 1.

III. JUSTIFICATION OF THE APPROXIMATE EQUALITY IN (5)

In this section, we would like to justify the approximate equality in (5). Assume that the sequence $\{Z_{B,2^k}(\mathbf{N})\}_{k=0}^\infty$ converges² to $Z_B(\mathbf{N})$. Then

$$\frac{Z(\mathbf{N})}{Z_B(\mathbf{N})} = \frac{Z(\mathbf{N})}{Z_{B,2}(\mathbf{N})} \cdot \frac{Z_{B,2}(\mathbf{N})}{Z_{B,4}(\mathbf{N})} \cdot \frac{Z_{B,4}(\mathbf{N})}{Z_{B,8}(\mathbf{N})} \cdot \frac{Z_{B,8}(\mathbf{N})}{Z_{B,16}(\mathbf{N})} \dots, \quad (10)$$

which holds thanks to the cancellation of terms on the RHS.

Let

$$\eta \triangleq \frac{Z(\mathbf{N})}{Z_{B,2}(\mathbf{N})} = \frac{Z_{B,1}(\mathbf{N})}{Z_{B,2}(\mathbf{N})},$$

²We suspect that $\limsup_{M \rightarrow \infty}$ in (2) can be replaced by $\lim_{M \rightarrow \infty}$ for general NFGs, but we are not aware of a proof of this.

and assume that we can show that

$$\frac{Z_{B,2}(N)}{Z_{B,4}(N)} \approx \eta^{1/2}, \quad \frac{Z_{B,4}(N)}{Z_{B,8}(N)} \approx \eta^{1/4}, \quad \dots \quad (11)$$

Then Eq. (10) can be rewritten as

$$\frac{Z(N)}{Z_B(N)} \approx \eta^{1/1} \cdot \eta^{1/2} \cdot \eta^{1/4} \cdot \eta^{1/8} \cdot \dots = \eta^2 = \left(\frac{Z(N)}{Z_{B,2}(N)} \right)^2,$$

which is exactly the claimed relationship in (5). Note that for for $M = 2^k$, where $k \in \mathbb{Z}_{\geq 0}$, Eq. (11) also implies

$$\frac{Z(N)}{Z_{B,M}(N)} \approx \eta^{2(1-1/M)} = \left(\frac{Z(N)}{Z_{B,2}(N)} \right)^{2(1-1/M)}. \quad (12)$$

Interestingly, the lower and upper bounds on $Z(N)/Z_{B,M}(N)$ in Eq. (10) of Theorem 4 in [8] are equal $\eta^{2(1-1/M)}$ for $\eta = 1$ and $\eta = 2^{n/4}$, respectively.

It remains to justify the expressions in (11). Indeed, the first expression in (11) follows from taking the fourth root on both sides of the equation

$$\frac{(Z_{B,2}(N))^4}{(Z_{B,4}(N))^4} = \frac{\langle Z(\tilde{N}) \rangle_{\tilde{N} \in \tilde{\mathcal{N}}_2}^2}{\langle Z(\tilde{N}) \rangle_{\tilde{N} \in \tilde{\mathcal{N}}_4}^2} \approx \frac{\langle Z(\tilde{N}) \rangle_{\tilde{N} \in \tilde{\mathcal{N}}_1}^2}{\langle Z(\tilde{N}) \rangle_{\tilde{N} \in \tilde{\mathcal{N}}_2}^2} = \frac{(Z_{B,1}(N))^2}{(Z_{B,2}(N))^2}.$$

Here, the approximation sign is justified as follows: the way 4-covers of N behave to 2-covers of N is similar to the way that 2-covers of N behave to 1-covers of N . (This is in general not an equality as not all 4-covers are 2-covers of 2-covers.) Similarly, the second expression in (11) follows from taking the eighth root on both sides of the equation

$$\frac{(Z_{B,4}(N))^8}{(Z_{B,8}(N))^8} = \frac{\langle Z(\tilde{N}) \rangle_{\tilde{N} \in \tilde{\mathcal{N}}_4}^2}{\langle Z(\tilde{N}) \rangle_{\tilde{N} \in \tilde{\mathcal{N}}_8}^2} \approx \frac{\langle Z(\tilde{N}) \rangle_{\tilde{N} \in \tilde{\mathcal{N}}_2}^2}{\langle Z(\tilde{N}) \rangle_{\tilde{N} \in \tilde{\mathcal{N}}_4}^2} = \frac{(Z_{B,2}(N))^4}{(Z_{B,4}(N))^4}.$$

Here, the approximation sign is justified as follows: the way 8-covers of N behave to 4-covers of N is similar to the way that 4-covers of N behave to 2-covers of N . (This is in general not an equality as not all 8-covers are 2-covers of 4-covers.) The justification for the remaining expressions in (11) is similar.

This concludes the proposed justification of the approximate equality in (5).

IV. ANALYSIS OF A SINGLE-CYCLE GRAPHICAL MODEL

Consider the NFG N in Fig. 4 that consists of a single function node f_1 of degree two and an edge e_1 with associated variable $A_{e_1} \in \{0, 1\}$. (The dot denotes the first argument of f_1 .) Let

$$\mathbf{T}_{f_1} \triangleq \begin{pmatrix} f_1(0, 0) & f_1(0, 1) \\ f_1(1, 0) & f_1(1, 1) \end{pmatrix}.$$

In order to keep the discussion simple, we assume that f_1 takes on strictly positive values.

Let λ_1 and λ_2 with $|\lambda_1| \geq |\lambda_2|$ be the two eigenvalues of \mathbf{T}_{f_1} . For the given setup we can use Perron-Frobenius theory to conclude that λ_1 and λ_2 are real numbers satisfying $\lambda_1 > |\lambda_2|$.

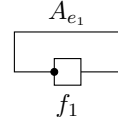


Fig. 4: NFG N discussed in Section IV. ■

Proposition 3. For the NFG N defined at the beginning of this section, it holds that

$$\begin{aligned} Z(N) &= \sum_{a_{e_1}} f_1(a_{e_1}, a_{e_1}) = \text{Tr}(\mathbf{T}_{f_1}) = \lambda_1 + \lambda_2, \\ Z_{B,2}(N) &= \sqrt{\frac{1}{2}(\text{Tr}(\mathbf{T}_{f_1}))^2 + \frac{1}{2}\text{Tr}((\mathbf{T}_{f_1})^2)} = \sqrt{\lambda_1^2 + \lambda_1 \lambda_2 + \lambda_2^2}, \\ Z_B(N) &= \lambda_1. \end{aligned}$$

Proof: See Appendix A. ■

Computing the ratio on the LHS of (7), we observe that

$$\rho(N) = \frac{Z(N) \cdot Z_B(N)}{(Z_{B,2}(N))^2} = \frac{\lambda_1^2 + \lambda_1 \lambda_2}{\lambda_1^2 + \lambda_1 \lambda_2 + \lambda_2^2} = 1 - \frac{\xi^2}{1 + \xi + \xi^2},$$

where $\xi \triangleq \lambda_2/\lambda_1$. We see that the smaller ξ is, the closer the ratio on the LHS of (7) is to one. In particular, if $|\xi + \xi^2| < 1$, then $\rho(N) = 1 - \xi^2 + \xi^3 + O(\xi^4)$.

Let θ be a real number satisfying $0 < \theta \leq 1$. Consider the special case where the function f_1 is such that $\mathbf{T}_{f_1} \triangleq \begin{pmatrix} 1 & \theta \\ \theta & 1 \end{pmatrix}$. Note that the function f_1 is log-supermodular. (For details of the definition of log-supermodularity, see, e.g., [9], [10].)

The eigenvalues of \mathbf{T}_{f_1} are $\lambda_1 = 1 + \theta$ and $\lambda_2 = 1 - \theta$, and so $\xi = \frac{\lambda_2}{\lambda_1} = \frac{1 - \theta}{1 + \theta}$. We observe that if θ is close to one, then ξ is close to zero, and with that the ratio $\rho(N)$ is close to one. On the other hand, if θ is close to zero, then ξ is close to one, and with that the ratio $\rho(N)$ is close to $2/3$.

V. ANALYSIS OF A SPECIAL CLASS OF LOG-SUPERMODULAR GRAPHICAL MODELS

A. Definition of a Special Class of Log-supermodular Graphical Models

Let θ be a real number satisfying $0 < \theta \leq 1$. Consider an NFG N with m function nodes and n (full) edges, where all function nodes have degree 3 and represent the local function

$$f_0(a_1, a_2, a_3) \triangleq \begin{cases} 1 & (\text{if } a_1 = a_2 = a_3) \\ \theta & (\text{otherwise}) \end{cases}$$

Note:

- The parameters m and n have to satisfy $3m = 2n$.
- The function f_0 is symmetric in the arguments. With this, the ordering of the arguments is irrelevant.
- The function f_0 is log-supermodular. (For details of the definition of log-supermodularity, see, e.g., [9], [10].)

B. The Bethe Approximation of the Partition Sum

Let us determine $Z_B(N)$ by finding the sum-product algorithm (SPA) fixed-point messages [4]. Because of the symmetry of the setup, we may assume that all the messages along all the edges in all directions are the same, say $\mu = (\mu(0), \mu(1)) = \frac{1}{\Lambda+1} \cdot (\Lambda, 1)$ for some $\Lambda \in \mathbb{R}_{\geq 0} \cup \{+\infty\}$.

Lemma 4. *If $1/5 \leq \theta \leq 1$, then the SPA has one fixed-point message corresponding to*

$$\Lambda_0 = 1.$$

Note that Λ_0 corresponds to a stable SPA fixed-point.

If $0 < \theta < 1/5$, then the SPA has three fixed-point messages corresponding to

$$\Lambda_0 = 1, \quad \Lambda_{\pm} = \frac{1}{2\theta} \cdot (1 - 3\theta \pm \sqrt{5\theta^2 - 6\theta + 1}).$$

Note that $\Lambda_- = \Lambda_+^{-1}$. Moreover, Λ_+ and Λ_- correspond to stable SPA fixed points, whereas Λ_0 corresponds to an unstable SPA fixed point.

Proof: See Appendix B. ■

Remark 5. *It follows from Lemma 4 that the Bethe approximation for the class of NFGs under consideration has a phase transition at $\theta^* = 1/5$.*

Proposition 6. *If $1/5 \leq \theta \leq 1$, then it holds that*

$$Z_B(N) = \frac{(2+6\theta)^m}{2^n} = \left(\frac{2+6\theta}{\sqrt{8}} \right)^m.$$

(We omit the corresponding expression for Z_B for the case $0 < \theta < 1/5$.)

Proof: The Bethe partition sum is given by

$$Z_B(N) = \frac{\prod_f Z_f}{\prod_e Z_e},$$

where the product in the numerator is over all function nodes, where the product in the denominator is over all full edges, and where, thanks to the fact that all the SPA fixed-point messages are the same, the expressions for Z_f and Z_e are given by

$$Z_f = \sum_{a_1, a_2, a_3} f_0(a_1, a_2, a_3) \mu(a_1) \mu(a_2) \mu(a_3),$$

$$Z_e = (\mu(0))^2 + (\mu(1))^2.$$

Using the results from Lemma 4, we obtain the result in the proposition statement. ■

C. Loop-Calculus Transform

It turns out that the loop-calculus approach by Chertkov and Chernyak [11] can be beneficially used to better understand the connection of $Z_B(N)$ and $Z(N)$ for the class of NFGs under consideration in this section. Here we apply the loop-calculus approach in terms of the loop-calculus transform (LCT) as defined in [12, Section VI.B] and obtain a new NFG N_{LCT}

with global function g_{LCT} . Let $f_{0,LCT}$ be the function node in N_{LCT} corresponding to f_0 .

Lemma 7. *If $1/5 \leq \theta \leq 1$, then the LCT based on $\Lambda = \Lambda_0$ yields*

$$f_{0,LCT}(a_1, a_2, a_3) = \begin{cases} \frac{2+6\theta}{\sqrt{8}} & (\text{if } (a_1, a_2, a_3) = (0, 0, 0)) \\ \frac{2-2\theta}{\sqrt{8}} & (\text{if } (a_1, a_2, a_3) = (0, 1, 1)) \\ \frac{2-2\theta}{\sqrt{8}} & (\text{if } (a_1, a_2, a_3) = (1, 0, 1)) \\ \frac{2-2\theta}{\sqrt{8}} & (\text{if } (a_1, a_2, a_3) = (1, 1, 0)) \\ 0 & (\text{otherwise}) \end{cases}$$

(We omit the corresponding expression for $0 < \theta < 1/5$ that is obtained by an LCT based on $\Lambda = \Lambda_+$, but we note that $f_{0,LCT}(a_1, a_2, a_3) > 0$ for $(a_1, a_2, a_3) = (1, 1, 1)$.)

Proof: Omitted. ■

Note that, by design of the LCT:

- $Z_B(N) = g_{LCT}(\mathbf{0}) = \prod_f f_{0,LCT}(0, 0, 0) \stackrel{(*)}{=} \left(\frac{2+6\theta}{\sqrt{8}} \right)^m$, where $(*)$ is for the case $1/5 \leq \theta \leq 1$.
- $Z(N) = \sum_{\mathbf{a}} g_{LCT}(\mathbf{a}) = Z_B(N) + \sum_{\mathbf{a} \neq \mathbf{0}} g_{LCT}(\mathbf{a})$.
- $f_{0,LCT}(a_1, a_2, a_3) = 0$ for $(a_1, a_2, a_3) = (1, 0, 0), (0, 1, 0), (0, 0, 1)$.

Remark 8. *Assume $1/5 \leq \theta \leq 1$. It follows from Lemma 7 that the valid configurations of N_{LCT} have a simple structure: the edges that take on the value 1 (more precisely, the edges whose associated variable takes on the value 1), form a cycle or a disjoint union of cycles. In fact, there is a bijection between the set of valid configurations of N_{LCT} and the set of codewords of a $(2, 3)$ -regular LDPC code \mathcal{C}_{LCT} whose Tanner graph is represented by N_{LCT} after inserting a variable node in every edge.³*

Lemma 9. *Let \mathbf{a} be a valid configuration of N_{LCT} , i.e., $\mathbf{a} \in \mathcal{C}_{LCT}$. Then it holds that*

$$g_{LCT}(\mathbf{a}) = Z_B(N) \cdot \left(\frac{2-2\theta}{2+6\theta} \right)^{w_H(\mathbf{a})},$$

where $w_H(\mathbf{a})$ is the Hamming weight of \mathbf{a} .

Proof: This result follows from the observation that a cycle visits equally many edges as function nodes. Similarly, a disjoint union of cycles visits equally many edges as function nodes. ■

Note that for $1/5 \leq \theta \leq 1$ it holds that $\frac{2-2\theta}{2+6\theta} \leq 1/2$. It follows from Lemma 9 that the larger $w_H(\mathbf{a})$ is, the smaller is the contribution of $g_{LCT}(\mathbf{a})$ to $\sum_{\mathbf{a}} g_{LCT}(\mathbf{a})$. Moreover,

$$Z(N) = Z_B(N) + \sum_{\mathbf{a} \in \mathcal{C}_{LCT} \setminus \{\mathbf{0}\}} g_{LCT}(\mathbf{a})$$

$$= Z_B(N) \cdot \left(1 + \underbrace{\sum_{\mathbf{a} \in \mathcal{C}_{LCT} \setminus \{\mathbf{0}\}} \left(\frac{2-2\theta}{2+6\theta} \right)^{w_H(\mathbf{a})}}_{(*)} \right).$$

³Because of their codeword structure, such codes are also known as cycle codes. (This is not to be confused with cyclic codes.)

Using well-known techniques for studying the expected Hamming weight distribution of regular LDPC codes (see, e.g., [13]; details are omitted), one can conclude that the expression in $(*)$ is typically at most on the order of 1, and so $Z_B(N)$ gives a (very) good approximation of $Z(N)$.

For the case $0 < \theta < 1/5$, similar conclusions can be reached, but the analysis is more elaborate as the set of valid configurations is larger.

D. Double-Cover Transform

In order to find $Z_{B,2}(N)$, we apply the double-cover analysis technique in [10]. Actually, we apply the technique in [10] not to N , but to N_{LCT} , resulting in a graphical model called $N_{LCT-DCT}$ with global function $g_{LCT-DCT}$ and variables that take value in $\{(0,0), (0,1), (1,0), (1,1)\}$. (Some details of the relevant calculations are given in Appendix C.)

For simplicity, we consider only the case $1/5 \leq \theta \leq 1$ in the following. We obtain

$$(Z_{B,2}(N))^2 = (Z_B(N))^2 \cdot \underbrace{\left(1 + \sum_{\hat{\mathbf{a}} \in \mathcal{C}_{LCT-DCT} \setminus \{\mathbf{0}\}} \frac{g_{LCT-DCT}(\hat{\mathbf{a}})}{(Z_B(N))^2}\right)}_{(**)}.$$

Compare this with

$$Z(N) \cdot Z_B(N) = (Z_B(N))^2 \cdot \underbrace{\left(1 + \sum_{\mathbf{a} \in \mathcal{C}_{LCT} \setminus \{\mathbf{0}\}} \frac{g_{LCT}(\mathbf{a})}{Z_B(N)}\right)}_{(***)}.$$

It turns out (details are omitted) that the dominating contribution to $(**)$ come from valid configurations that correspond to $(0,1)$ -cycles and disjoint unions of $(0,1)$ -cycles. Moreover, there is not only a bijection between these valid configurations in $(**)$ and the valid configurations in $(***)$, but also their global function value (normalized by $(Z_B(N))^2$ and $Z_B(N)$, respectively) is the same. With this, the relationship

$$Z(N) \cdot Z_B(N) \approx (Z_{B,2}(N))^2$$

is not too surprising for the NFG under consideration.

E. Numerical Results

We consider a particular instance of the class of graphical models under consideration in this section. Namely, let N have $m = 8$ function nodes, $n = 12$ edges, and let its graph structure be described by the (randomly generated) incidence matrix \mathbf{H} shown in Appendix D, where the 8 rows and 12 columns of \mathbf{H} correspond to, respectively, the 8 function nodes and the 12 edges of N . Note that \mathbf{H} happens to be the parity-check matrix of the $(2,3)$ -regular LDPC code \mathcal{C}_{LCT} . Fig. 5 shows $\log_2(Z(N))$, $\log_2(Z_{B,2}(N))$, and $\log_2(Z_B(N))$ as a function of the parameter θ . We make the following observations:

- For $0.4 \lesssim \theta \leq 1$, the Bethe approximation $Z_B(N)$ is very close to the partition sum $Z(N)$.
- For all values of θ , the blue curve for $\log_2(Z_{B,2}(N))$ is roughly half the way between the red curve for

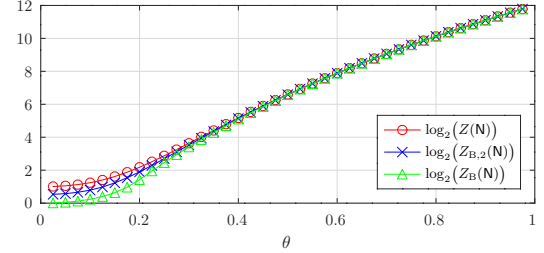


Fig. 5: Numerical results for NFG N discussed in Section V-E.

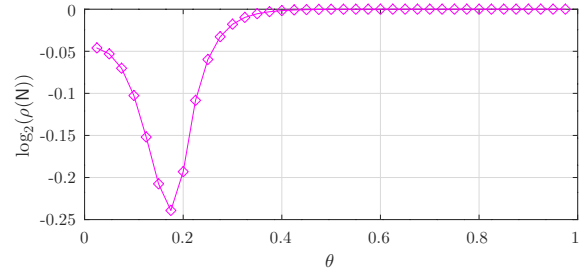


Fig. 6: Numerical results for NFG N discussed in Section V-E.

$\log_2(\rho(N))$ and the green curve for $\log_2(Z_B(N))$, thereby showing that $\rho(N) \approx 1$, where $\rho(N)$ was defined in (7). Fig. 6 considers the value of $\log_2(\rho(N))$ as a function of θ . We make the following observations:

- For $0.4 \lesssim \theta \leq 1$, the ratio $\rho(N)$ is very close to one.
- Interestingly, the ratio $\rho(N)$ is the furthest from 1 when θ is close to the phase transition point $\theta^* = 1/5$. (Note that $2^{-0.25} \approx 0.841$.)

Finally, note that Ruozzi [9] showed that for any log-supermodular NFG N , any positive integer M , and any $\tilde{N} \in \tilde{\mathcal{N}}_M$, it holds that $Z(\tilde{N}) \leq Z(N)^M$. For the class of log-supermodular NFGs under consideration in this section we can significantly strengthen this result for $M = 2$. Namely, for most $\tilde{N} \in \tilde{\mathcal{N}}_2$ it holds that $Z(\tilde{N})$ is very close to $Z(N)^2$.

VI. CONCLUSION

A first key result of this paper is the approximate equality in (5) and its justification in Section III. It remains to be seen to what extent the approximation in this equation can be turned into a rigorous mathematical statement, at least for some classes of NFGs.

Another key result of this paper was to show how the loop-calculus transform (LCT) and the double-cover transform (DCT) can be combined to yield insightful results about the relationship of $Z(N)$, $Z_{B,2}(N)$, and $Z_B(N)$ in general, and the ratio $\rho(N)$ in particular, for the specific class of log-supermodular NFGs under consideration in Section V.

It remains to be seen what techniques can be used to obtain results about $Z(N)$, $Z_{B,2}(N)$, $Z_B(N)$, and $\rho(N)$ for other classes of NFGs, e.g., the NFGs in [14]–[16].

APPENDIX A PROOF OF PROPOSITION 3

The result for $Z(N)$ is straightforward.

The result for $Z_{B,2}(N)$ follows from the observation that the NFG N in Fig. 4 has two double covers:

- One double cover consists of two independent copies of N , resulting in a contribution of $(\text{Tr}(\mathbf{T}_{f_1}))^2$ to $(Z_{B,2}(N))^2$.
- One double cover consists of a single cycle where the function node f_1 appears twice in sequence, resulting in a contribution of $\text{Tr}((\mathbf{T}_{f_1})^2)$ to $(Z_{B,2}(N))^2$.

The result for $Z_B(N)$ follows from the observation that the right Perron eigenvector of \mathbf{T}_{f_1} forms an SPA fixed-point message for the message going in the clockwise direction of the cycle in the NFG N in Fig. 4, whereas the left Perron eigenvector of \mathbf{T}_{f_1} forms an SPA fixed-point message for the message going in the counter-clockwise direction of the cycle in the NFG N in Fig. 4.

APPENDIX B PROOF OF LEMMA 4

From the definition of f_0 , it follows that the SPA fixed-point messages have to satisfy

$$\frac{\mu(0)}{\mu(1)} = \frac{f_0(0,0,0)\mu(0)\mu(0) + f_0(0,0,1)\mu(0)\mu(1)}{f_0(0,1,0)\mu(1)\mu(0) + f_0(0,1,1)\mu(1)\mu(1)} = \frac{f_0(1,0,0)\mu(0)\mu(0) + f_0(1,0,1)\mu(0)\mu(1)}{f_0(1,1,0)\mu(1)\mu(0) + f_0(1,1,1)\mu(1)\mu(1)}.$$

Using the definitions of Λ and f_0 , this equation becomes

$$\Lambda = \frac{\Lambda^2 + 2\theta\Lambda + \theta}{\theta\Lambda^2 + 2\theta\Lambda + 1},$$

which can be rewritten as

$$\Lambda^3 + (2-\theta^{-1})\Lambda^2 + (\theta^{-1}-2)\Lambda - 1 = 0. \quad (13)$$

It turns out that $\Lambda = 1$ is always a root of (13). With this, Eq. (13) can be rewritten as

$$(\Lambda - 1) \cdot \underbrace{(\Lambda^2 + (3-\theta^{-1})\Lambda + 1)}_{(*)} = 0.$$

The above observations allow us to draw the following conclusions.

- If $0 < \theta < 1/5$, then the discriminant of the quadratic polynomial in $(*)$ is positive and we obtain the solutions mentioned in the lemma statement.
- If $\theta = 1/5$, then the discriminant of the quadratic polynomial in $(*)$ is zero. Given that $\Lambda = 1$ is a zero of multiplicity two of $(*)$, it turns out that $\Lambda = 1$ is a triple root of (13).
- If $1/5 < \theta \leq 1$, then the discriminant of the quadratic polynomial in $(*)$ is negative and $\Lambda = 1$ is the only real root of (13).

APPENDIX C SOME DETAILS OF THE CALCULATIONS IN SECTION V-D

The technique that we are using is explained in Sections III and IV of [10]; we refer to that paper for all the details. Here we will only show the key results from Section IV.B of [10].

Namely, for a local function f with three arguments that take value in $\{0, 1\}$, the analysis technique in [10] introduces a local function \hat{f} with three arguments that take value in $\{(0, 0), (0, 1), (1, 0), (1, 1)\}$. The $4 \times 4 \times 4$ array $\mathbf{T}_{\hat{f}}$ associated with \hat{f} is given by

$$\begin{array}{c|c|c|c} t_{000}t_{000} & \sqrt{2}t_{000}t_{010} & 0 & t_{010}t_{010} \\ \hline \sqrt{2}t_{000}t_{100} & \text{perm}(\mathbf{T}_{f|a_3=0}) & 0 & \sqrt{2}t_{010}t_{110} \\ 0 & 0 & \det(\mathbf{T}_{f|a_3=0}) & 0 \\ \hline t_{100}t_{100} & \sqrt{2}t_{100}t_{110} & 0 & t_{110}t_{110} \end{array},$$

$$\begin{array}{c|c|c|c} \sqrt{2}t_{000}t_{001} & \text{perm}(\mathbf{T}_{f|a_1=0}) & 0 & \sqrt{2}t_{010}t_{011} \\ \hline \text{perm}(\mathbf{T}_{f|a_2=0}) & \hat{f}(\hat{0}, \hat{0}, \hat{0}) & 0 & \text{perm}(\mathbf{T}_{f|a_2=1}) \\ 0 & 0 & \hat{f}(\hat{1}, \hat{1}, \hat{0}) & 0 \\ \hline \sqrt{2}t_{100}t_{101} & \text{perm}(\mathbf{T}_{f|a_1=1}) & 0 & \sqrt{2}t_{110}t_{111} \end{array},$$

$$\begin{array}{c|c|c|c} 0 & 0 & \det(\mathbf{T}_{f|a_1=0}) & 0 \\ \hline 0 & 0 & \hat{f}(\hat{0}, \hat{1}, \hat{1}) & 0 \\ \hline \det(\mathbf{T}_{f|a_2=0}) & \hat{f}(\hat{1}, \hat{0}, \hat{1}) & 0 & \det(\mathbf{T}_{f|a_2=1}) \\ \hline 0 & 0 & \det(\mathbf{T}_{f|a_1=1}) & 0 \end{array},$$

$$\begin{array}{c|c|c|c} t_{001}t_{001} & \sqrt{2}t_{001}t_{011} & 0 & t_{011}t_{011} \\ \hline \sqrt{2}t_{001}t_{101} & \text{perm}(\mathbf{T}_{f|a_3=1}) & 0 & \sqrt{2}t_{011}t_{111} \\ 0 & 0 & \det(\mathbf{T}_{f|a_3=1}) & 0 \\ \hline t_{101}t_{101} & \sqrt{2}t_{101}t_{111} & 0 & t_{111}t_{111} \end{array}.$$

Here:

- The rows of the above matrices are indexed by $\{(0, 0), (0, 1), (1, 0), (1, 1)\}$ and correspond to the values taken by the first argument of \hat{f} .
- The columns of the above matrices are indexed by $\{(0, 0), (0, 1), (1, 0), (1, 1)\}$ and correspond to the values taken by the second argument of \hat{f} .
- The above four matrices are indexed by $\{(0, 0), (0, 1), (1, 0), (1, 1)\}$ and correspond to the values taken by the third argument of \hat{f} .
- $t_{000} \triangleq f(0, 0, 0)$, $t_{001} \triangleq f(0, 0, 1)$, etc.
- $\mathbf{T}_{f|a_3=0}$ and $\mathbf{T}_{f|a_3=1}$ are the matrices associated with the functions $f(a_1, a_2, 0)$ and $f(a_1, a_2, 1)$, respectively. The matrices $\mathbf{T}_{f|a_1=0}$, $\mathbf{T}_{f|a_1=1}$, $\mathbf{T}_{f|a_2=0}$, and $\mathbf{T}_{f|a_2=1}$ are defined analogously.
- $\hat{0} \triangleq (0, 1)$, $\hat{1} \triangleq (1, 0)$, and $\gamma \triangleq 1/\sqrt{2}$.
- $\hat{f}(\hat{0}, \hat{0}, \hat{0}) = \gamma \cdot (t_{000}t_{111} + t_{100}t_{011} + t_{010}t_{101} + t_{001}t_{110})$.
- $\hat{f}(\hat{1}, \hat{0}, \hat{0}) = \gamma \cdot (t_{000}t_{111} - t_{100}t_{011} + t_{010}t_{101} - t_{001}t_{110})$.
- $\hat{f}(\hat{0}, \hat{1}, \hat{0}) = \gamma \cdot (t_{000}t_{111} + t_{100}t_{011} - t_{010}t_{101} - t_{001}t_{110})$.
- $\hat{f}(\hat{1}, \hat{1}, \hat{0}) = \gamma \cdot (t_{000}t_{111} - t_{100}t_{011} - t_{010}t_{101} + t_{001}t_{110})$.

(The above $4 \times 4 \times 4$ array corrects a few minor typos in the corresponding array in [10].)

(continued on the next page)

The above result was for an arbitrary local function f with three arguments each taking values in $\{0, 1\}$. If f is the result of an LCT, then $f(1, 0, 0) = t_{100} = 0$, $f(0, 1, 0) = t_{010} = 0$, $f(0, 0, 1) = t_{001} = 0$, and the above $4 \times 4 \times 4$ array $\mathbf{T}_{\hat{f}}$ simplifies to

$$\begin{aligned} & \left(\begin{array}{c|ccc} t_{000}t_{000} & 0 & 0 & 0 \\ \hline 0 & t_{000}t_{110} & 0 & 0 \\ 0 & 0 & t_{000}t_{110} & 0 \\ \hline 0 & 0 & 0 & t_{110}t_{110} \end{array} \right), \\ & \left(\begin{array}{c|ccc} 0 & t_{000}t_{011} & 0 & 0 \\ \hline t_{000}t_{101} & \sqrt{2}^{-1}t_{000}t_{111} & 0 & t_{011}t_{110} \\ 0 & 0 & \sqrt{2}^{-1}t_{000}t_{111} & 0 \\ \hline 0 & t_{101}t_{110} & 0 & \sqrt{2}t_{110}t_{111} \end{array} \right), \\ & \left(\begin{array}{c|ccc} 0 & 0 & t_{000}t_{011} & 0 \\ \hline 0 & 0 & \sqrt{2}^{-1}t_{000}t_{111} & 0 \\ t_{000}t_{101} & \sqrt{2}^{-1}t_{000}t_{111} & 0 & -t_{011}t_{110} \\ \hline 0 & 0 & -t_{101}t_{110} & 0 \end{array} \right), \\ & \left(\begin{array}{c|ccc} 0 & 0 & 0 & t_{011}t_{011} \\ \hline 0 & t_{011}t_{101} & 0 & \sqrt{2}t_{011}t_{111} \\ 0 & 0 & -t_{011}t_{101} & 0 \\ \hline t_{101}t_{101} & \sqrt{2}t_{101}t_{111} & 0 & t_{111}t_{111} \end{array} \right). \end{aligned}$$

It follows from the derivations in [10] that function values of \hat{f} where at least one of the arguments equals $(1, 0)$ do not appear in the calculation of $Z_{B,2}(N)$. With this, the above $4 \times 4 \times 4$ array $\mathbf{T}_{\hat{f}}$ can be further simplified to

$$\begin{aligned} & \left(\begin{array}{c|ccc} t_{000}t_{000} & 0 & 0 & 0 \\ \hline 0 & t_{000}t_{110} & 0 & 0 \\ 0 & 0 & 0 & 0 \\ \hline 0 & 0 & 0 & t_{110}t_{110} \end{array} \right), \\ & \left(\begin{array}{c|ccc} 0 & t_{000}t_{011} & 0 & 0 \\ \hline t_{000}t_{101} & \sqrt{2}^{-1}t_{000}t_{111} & 0 & t_{011}t_{110} \\ 0 & 0 & 0 & 0 \\ \hline 0 & t_{101}t_{110} & 0 & \sqrt{2}t_{110}t_{111} \end{array} \right), \\ & \left(\begin{array}{c|ccc} 0 & 0 & 0 & 0 \\ \hline 0 & 0 & 0 & 0 \\ 0 & 0 & 0 & 0 \\ \hline 0 & 0 & 0 & 0 \end{array} \right), \\ & \left(\begin{array}{c|ccc} 0 & 0 & 0 & t_{011}t_{011} \\ \hline 0 & t_{011}t_{101} & 0 & \sqrt{2}t_{011}t_{111} \\ 0 & 0 & 0 & 0 \\ \hline t_{101}t_{101} & \sqrt{2}t_{101}t_{111} & 0 & t_{111}t_{111} \end{array} \right). \end{aligned}$$

Finally, let us show the last two $4 \times 4 \times 4$ arrays for the special case where $f(1, 1, 1) = t_{111} = 0$. We obtain

$$\begin{aligned} & \left(\begin{array}{c|ccc} t_{000}t_{000} & 0 & 0 & 0 \\ \hline 0 & t_{000}t_{110} & 0 & 0 \\ 0 & 0 & t_{000}t_{110} & 0 \\ \hline 0 & 0 & 0 & t_{110}t_{110} \end{array} \right), \\ & \left(\begin{array}{c|ccc} 0 & t_{000}t_{011} & 0 & 0 \\ \hline t_{000}t_{101} & 0 & 0 & t_{011}t_{110} \\ 0 & 0 & 0 & 0 \\ \hline 0 & t_{101}t_{110} & 0 & 0 \end{array} \right), \\ & \left(\begin{array}{c|ccc} 0 & 0 & t_{000}t_{011} & 0 \\ \hline 0 & 0 & 0 & 0 \\ t_{000}t_{101} & 0 & 0 & -t_{011}t_{110} \\ \hline 0 & 0 & -t_{101}t_{110} & 0 \end{array} \right), \\ & \left(\begin{array}{c|ccc} 0 & 0 & 0 & t_{011}t_{011} \\ \hline 0 & t_{011}t_{101} & 0 & 0 \\ 0 & 0 & -t_{011}t_{101} & 0 \\ \hline t_{101}t_{101} & 0 & 0 & 0 \end{array} \right) \end{aligned}$$

and

$$\begin{aligned} & \left(\begin{array}{c|ccc} t_{000}t_{000} & 0 & 0 & 0 \\ \hline 0 & t_{000}t_{110} & 0 & 0 \\ 0 & 0 & 0 & 0 \\ \hline 0 & 0 & 0 & t_{110}t_{110} \end{array} \right), \\ & \left(\begin{array}{c|ccc} 0 & t_{000}t_{011} & 0 & 0 \\ \hline t_{000}t_{101} & 0 & 0 & t_{011}t_{110} \\ 0 & 0 & 0 & 0 \\ \hline 0 & t_{101}t_{110} & 0 & 0 \end{array} \right), \\ & \left(\begin{array}{c|ccc} 0 & 0 & 0 & 0 \\ \hline 0 & 0 & 0 & 0 \\ 0 & 0 & 0 & 0 \\ \hline 0 & 0 & 0 & 0 \end{array} \right), \\ & \left(\begin{array}{c|ccc} 0 & 0 & 0 & t_{011}t_{011} \\ \hline 0 & t_{011}t_{101} & 0 & 0 \\ 0 & 0 & 0 & 0 \\ \hline t_{101}t_{101} & 0 & 0 & 0 \end{array} \right). \end{aligned}$$

In particular, for the function $f_{0,LCT}$ in Lemma 7 we obtain

$$\begin{aligned} & \left(\begin{array}{c|ccc} \alpha^2 & 0 & 0 & 0 \\ \hline 0 & \alpha\beta & 0 & 0 \\ 0 & 0 & 0 & 0 \\ \hline 0 & 0 & 0 & \beta^2 \end{array} \right), \\ & \left(\begin{array}{c|ccc} 0 & \alpha\beta & 0 & 0 \\ \hline \alpha\beta & 0 & 0 & \beta^2 \\ 0 & 0 & 0 & 0 \\ \hline 0 & \beta^2 & 0 & 0 \end{array} \right), \\ & \left(\begin{array}{c|ccc} 0 & 0 & 0 & 0 \\ \hline 0 & 0 & 0 & 0 \\ 0 & 0 & 0 & 0 \\ \hline 0 & 0 & 0 & 0 \end{array} \right), \\ & \left(\begin{array}{c|ccc} 0 & 0 & 0 & \beta^2 \\ \hline 0 & \beta^2 & 0 & 0 \\ 0 & 0 & 0 & 0 \\ \hline \beta^2 & 0 & 0 & 0 \end{array} \right), \end{aligned}$$

where $\alpha \triangleq \frac{2+6\theta}{\sqrt{8}}$ and $\beta \triangleq \frac{2-2\theta}{\sqrt{8}}$. Analyzing the support of the function \hat{f} , yields some of the results mentioned in Section V-D.

APPENDIX D

INCIDENCE MATRIX USED IN SECTION V-E

The incidence matrix used in Section V-E is

$$\mathbf{H} = \begin{pmatrix} 0 & 0 & 0 & 0 & 0 & 0 & 0 & 0 & 1 & 1 & 0 & 1 \\ 0 & 0 & 1 & 0 & 0 & 0 & 0 & 1 & 0 & 0 & 1 & 0 \\ 0 & 0 & 1 & 0 & 0 & 1 & 0 & 0 & 1 & 0 & 0 & 0 \\ 0 & 0 & 0 & 0 & 1 & 1 & 1 & 0 & 0 & 0 & 0 & 0 \\ 1 & 1 & 0 & 0 & 1 & 0 & 0 & 0 & 0 & 0 & 0 & 0 \\ 1 & 0 & 0 & 0 & 0 & 0 & 0 & 0 & 0 & 0 & 1 & 1 \\ 0 & 0 & 0 & 1 & 0 & 0 & 0 & 1 & 0 & 1 & 0 & 0 \\ 0 & 1 & 0 & 1 & 0 & 0 & 1 & 0 & 0 & 0 & 0 & 0 \end{pmatrix}.$$

REFERENCES

- [1] F. R. Kschischang, B. J. Frey, and H.-A. Loeliger, “Factor graphs and the sum-product algorithm,” *IEEE Trans. Inf. Theory*, vol. 47, no. 2, pp. 498–519, Feb. 2001.
- [2] G. D. Forney, Jr., “Codes on graphs: normal realizations,” *IEEE Trans. Inf. Theory*, vol. 47, no. 2, pp. 520–548, Feb. 2001.
- [3] H.-A. Loeliger, “An introduction to factor graphs,” *IEEE Sig. Proc. Mag.*, vol. 21, no. 1, pp. 28–41, Jan. 2004.
- [4] J. S. Yedidia, W. T. Freeman, and Y. Weiss, “Constructing free-energy approximations and generalized belief propagation algorithms,” *IEEE Trans. Inf. Theory*, vol. 51, no. 7, pp. 2282–2312, Jul. 2005.
- [5] P. O. Vontobel, “Counting in graph covers: a combinatorial characterization of the Bethe entropy function,” *IEEE Trans. Inf. Theory*, vol. 59, no. 9, pp. 6018–6048, Sep. 2013.
- [6] ———, “The Bethe permanent of a non-negative matrix,” *IEEE Trans. Inf. Theory*, vol. 59, no. 3, pp. 1866–1901, Mar. 2013.
- [7] K. S. Ng and P. O. Vontobel, “Double-cover-based analysis of the Bethe permanent of non-negative matrices,” in *Proc. IEEE Inf. Theory Workshop*, Mumbai, India, Nov. 1–9 2022, pp. 1–6.
- [8] Y. Huang, N. Kashyap, and P. O. Vontobel, “Degree- M Bethe and Sinkhorn permanent based bounds on the permanent of a non-negative matrix,” *IEEE Trans. Inf. Theory*, vol. 70, no. 7, pp. 5289–5308, Jul. 2024.
- [9] N. Ruozzi, “The Bethe partition function of log-supermodular graphical models,” in *Proc. Neural Inf. Proc. Sys. Conf.*, Lake Tahoe, NV, USA, Dec. 3–6 2012.
- [10] P. O. Vontobel, “Analysis of double covers of factor graphs,” in *Proc. Int. Conf. Sig. Proc. and Comm.*, Bangalore, India, June 12–15 2016, pp. 1–5.
- [11] M. Chertkov and V. Y. Chernyak, “Loop series for discrete statistical models on graphs,” *J. Stat. Mech.: Theory and Experiment*, p. P06009, Jun. 2006.
- [12] G. D. Forney, Jr. and P. O. Vontobel, “Partition functions of normal factor graphs,” in *Proc. Inf. Theory Appl. Workshop*, UC San Diego, La Jolla, CA, USA, Feb. 6–11 2011.
- [13] T. Richardson and R. Urbank, *Modern Coding Theory*. New York, NY: Cambridge University Press, 2008.
- [14] D. Straszak and N. K. Vishnoi, “Belief propagation, Bethe approximation, and polynomials,” *IEEE Trans. Inf. Theory*, vol. 65, no. 7, pp. 4353–4363, Jul. 2019.
- [15] P. Csikvári, N. Ruozzi, and S. Shams, “Markov random fields, homomorphism counting, and Sidorenko’s conjecture,” *IEEE Trans. Inf. Theory*, vol. 68, no. 9, pp. 6052–6062, 2022.
- [16] Y. Huang and P. O. Vontobel, “The Bethe partition function and the SPA for factor graphs based on homogeneous real stable polynomials,” in *Proc. IEEE Int. Symp. Inf. Theory*, Athens, Greece, Jul. 7–12 2024, pp. 3029–3034.